



# **A model for establishment, maintenance and reactivation of the immune response after vaccination against Ebola virus**

Irène Balelli, Chloé Pasin, Melanie Prague, F. Crauste, T. V. Effelterre, V. Bockstal, L. Solforosi, Rodolphe Thiébaud

## **► To cite this version:**

Irène Balelli, Chloé Pasin, Melanie Prague, F. Crauste, T. V. Effelterre, et al.. A model for establishment, maintenance and reactivation of the immune response after vaccination against Ebola virus. *Journal of Theoretical Biology*, 2020, 495, pp.110254. hal-03160892v1

**HAL Id: hal-03160892**

**<https://hal.science/hal-03160892v1>**

Submitted on 5 Mar 2021 (v1), last revised 24 Jun 2020 (v2)

**HAL** is a multi-disciplinary open access archive for the deposit and dissemination of scientific research documents, whether they are published or not. The documents may come from teaching and research institutions in France or abroad, or from public or private research centers.

L'archive ouverte pluridisciplinaire **HAL**, est destinée au dépôt et à la diffusion de documents scientifiques de niveau recherche, publiés ou non, émanant des établissements d'enseignement et de recherche français ou étrangers, des laboratoires publics ou privés.



Distributed under a Creative Commons Attribution - NonCommercial - NoDerivatives 4.0 International License



# A model for establishment, maintenance and reactivation of the immune response after vaccination against Ebola virus

Irene Balelli<sup>a,b,c,\*</sup>, Chloé Pasin<sup>a,b,c,d</sup>, Mélanie Prague<sup>a,b,c</sup>, Fabien Crauste<sup>e</sup>, Thierry Van Effelterre<sup>f</sup>, Viki Bockstal<sup>g</sup>, Laura Solforsoli<sup>g</sup>, Rodolphe Thiébaud<sup>a,b,c</sup>

<sup>a</sup>INSERM U1219 Bordeaux Population Health, Université de Bordeaux, Bordeaux, France

<sup>b</sup>INRIA SISTM team, Talence, France

<sup>c</sup>Vaccine Research Institute, Créteil, France

<sup>d</sup>Department of Pathology and Cell Biology, Columbia University Medical Center, New York, New York, USA

<sup>e</sup>Université de Bordeaux, CNRS, Bordeaux INP, IMB, UMR 5251, F-33400 Talence, France

<sup>f</sup>Janssen Pharmaceutica N.V., Beerse, Belgium

<sup>g</sup>Janssen Vaccines & Prevention B.V., Leiden, The Netherlands

## ARTICLE INFO

### Article history:

Received 18 November 2019

Revised 17 March 2020

Accepted 18 March 2020

Available online 21 March 2020

### Keywords:

Mechanistic modeling

Immunological memory

Vaccination

Ebola virus

Identifiability analysis

Sensitivity analysis

Calibration

Heterologous vaccination

## ABSTRACT

The 2014–2016 Ebola outbreak in West Africa has triggered accelerated development of several preventive vaccines against Ebola virus. Under the EBOVAC1 consortium, three phase I studies were carried out to assess safety and immunogenicity of a two-dose heterologous vaccination regimen developed by Janssen Vaccines and Prevention in collaboration with Bavarian Nordic. To describe the immune response induced by the two-dose heterologous vaccine regimen, we propose a mechanistic ODE based model, which takes into account the role of immunological memory. We perform identifiability and sensitivity analysis of the proposed model to establish which kind of biological data are ideally needed in order to accurately estimate parameters, and additionally, which of those are non-identifiable based on the available data. Antibody concentrations data from phase I studies have been used to calibrate the model and show its ability in reproducing the observed antibody dynamics. Together with other factors, the establishment of an effective and reactive immunological memory is of pivotal importance for several prophylactic vaccines. We show that introducing a memory compartment in our calibrated model allows to evaluate the magnitude of the immune response induced by a booster dose and its long-term persistence afterwards.

© 2020 The Author(s). Published by Elsevier Ltd.

This is an open access article under the CC BY-NC-ND license.

(<http://creativecommons.org/licenses/by-nc-nd/4.0/>)

## 1. Introduction

Since the discovery of Ebola virus in 1976, recurring Ebola outbreaks have been recorded in equatorial Africa (Team, 2016; World Health Organisation, 2018). The largest outbreak ever recorded has affected West Africa between March 2014 and June 2016 (Organization et al., 2016), during which a Public Health Emergency of International Concern was declared, and resulted in more than 28,000 cases and 11,000 deaths, since no licensed vaccines nor cure were available. On August 1<sup>st</sup> 2018 a new Ebola outbreak

was declared in the Democratic Republic of Congo (DRC) in North Kivu and Ituri provinces (Organization et al., 2018). At present, it has been confined to a relatively small area but has already caused more than 3400 confirmed cases and 2250 confirmed deaths updated to March 1<sup>st</sup> 2020 (World Health Organisation, 2019a); the World Health Organization (WHO) declared a Public Health Emergency of International Concern on July 17<sup>th</sup> 2019 (World Health Organisation, 2019b).

Ebola virus (EBOV) belongs to the Filoviridae family, which includes five well-known species (Zaire (ZEBOV), Bundibugyo, Sudan, Reston and Tai Forest), and the recently discovered Bombali species (Goldstein et al., 2018). Ebola virus causes Ebola Viral Disease (EVD), a severe and acute illness, with a mortality rate ranging from 25% to 90% according to the WHO (World Health Organisation, 2018). Therefore, there is an urgent need for licensed Ebola vaccines.

\* Corresponding author at: 146 rue Léo-Saignat, 33076 BORDEAUX, France.

E-mail addresses: [irene.balelli@u-bordeaux.fr](mailto:irene.balelli@u-bordeaux.fr) (I. Balelli), [cgp2121@cumc.columbia.edu](mailto:cgp2121@cumc.columbia.edu) (C. Pasin), [melanie.prague@u-bordeaux.fr](mailto:melanie.prague@u-bordeaux.fr) (M. Prague), [fabien.crauste@u-bordeaux.fr](mailto:fabien.crauste@u-bordeaux.fr) (F. Crauste), [tvaneffe@ITSJNJ.com](mailto:tvaneffe@ITSJNJ.com) (T.V. Effelterre), [vbocksta@itsjnj.com](mailto:vbocksta@itsjnj.com) (V. Bockstal), [lsolforo@itsjnj.com](mailto:lsolforo@itsjnj.com) (L. Solforsoli), [rodolphe.thiebaud@u-bordeaux.fr](mailto:rodolphe.thiebaud@u-bordeaux.fr) (R. Thiébaud).

In response to the 2014–2016 Ebola outbreak, the development of several vaccine candidates against Ebola virus has been accelerated, with various vaccine platforms and antigen inserts (Gross et al., 2018; Venkatraman et al., 2018). In this context, in December 2014 the EBOVAC1 consortium was built under the Innovative Medicines Initiative Ebola+ Program. Its purpose was to support the development by Janssen Vaccines & Prevention B.V. of a new two-dose heterologous vaccine regimen against Ebola based on Adenovirus serotype 26 (Ad26.ZEBOV) and Modified Vaccinia Ankara (MVA-BN-Filo) vectors (Eurosurveillance editorial team, 2015). Ad26.ZEBOV vector encodes the glycoprotein (GP) of the Ebola Zaire virus, while MVA-BN-Filo encodes GPs from Ebola Zaire virus, Ebola Sudan virus, Marburg virus, and Tai Forest virus nucleoprotein.

The proposed two-dose regimens utilize both vaccines, administered at 28 or 56 days intervals. Three phase I studies have been carried out in four countries under EBOVAC1: United Kingdom (Milligan et al., 2016; Winslow et al., 2017), Kenya (Mutua et al., 2019), Uganda and Tanzania (Anywaine et al., 2019). The immune response following vaccination has been evaluated up to one year after the first dose through GP-specific binding antibody concentrations. Neutralizing antibody and T cell responses have also been evaluated up to one year of follow-up. Although human efficacy data are not available, results on non-human primate models have shown that the antibody concentration after the challenge correlates best with survival upon intramuscular challenge with Ebola virus (Sullivan et al., 2009; Wong et al., 2012; Dye et al., 2012; Calendret et al., 2018).

Therefore, it becomes relevant to estimate the persistence of the antibody response induced by the two-dose heterologous vaccine. The *in silico* approach we propose here will provide a good starting point to predict the humoral immune response elicited by the proposed vaccination regimen beyond the available persistence immunogenicity data.

The goal of prophylactic vaccination is to induce immunity against an infectious disease. Henceforth, it aims at stimulating the immune system and its ability to store and recall information about a specific pathogen, leading to a long-term protective immunity. This is possible by means of immunological memory, one of the core features of adaptive immune response (Pulendran and Ahmed, 2006; Hviid et al., 2015; Farber et al., 2016).

By generating specific antibodies, B cells play a key role in the mammalian adaptive immune system, and help protecting the organism against antigenic challenges. Several populations of specific B cells are generated upon antigen stimulation, with distinct functional roles. Naïve B cells become activated through the encounter with the antigen in secondary lymphoid organs. Upon activation, they can either become short-lived Antibody Secreting Cells (ASCs), or seed highly dynamic environments called Germinal Centers (GCs). In the second circumstance, B cells undergo B cell receptor (BCR) affinity maturation to improve their affinity against the presented antigen. The interaction of B cells with follicular dendritic cells and follicular helper T cells within GCs allows selection of B cells with improved antigen-binding ability (Inoue et al., 2018). During the course of a GC reaction, B cells can become either memory B cells or long-lived ASCs depending on the strength of their affinity. In particular, long-lived ASCs are generated after extensive B cells affinity maturation and produce high affinity antibodies. In contrast, memory B cells undergo less extensive affinity maturation, making them promptly available. Ultimately, ASCs are differentiated B cells able to produce high-affinity antibodies (Inoue et al., 2018; Victora and Nussenzweig, 2012; De Silva and Klein, 2015).

The primary infection induces a transient antibody response, because it is mostly characterized by short-lived ASCs. Indeed, findings on the kinetics of circulating ASCs following vaccination

show an early peak located around 7 days after vaccination, followed by a rapid relaxation phase: their level becomes undetectable after 10 to 14 days (Carter et al., 2017; Halliley et al., 2010; Leach et al., 2013). Nevertheless, the primary infection is able to elicit memory B cells, which play a key role in protection against subsequent infections with the same pathogen. Indeed, secondary exposure to a priming antigen is characterized by a more rapid and intense humoral response, which is of better quality as well (i.e. higher affinity antibodies) (Ademokun and Dunn-Walters, 2010; Tangye et al., 2003): this is the so called anamnestic response. Memory B cells can directly differentiate into short-lived ASCs, as well as seed new GCs for further affinity maturation (Inoue et al., 2018; Shlomchik, 2018). This is done in a more effective way than naïve B cells: it has been experimentally observed that memory B cells possess an intrinsic advantage over naïve B cells in both the time to initiate a response and in the division-based rate of effector cell development (Tangye et al., 2003). Once the infection has been controlled, the generated population of specific B cells contracts, leaving memory B cells and long-lived ASCs. The latter population partially migrates to the bone-marrow and assures long-term production of high-affinity antibodies (Halliley et al., 2015; Hammarlund et al., 2017).

Mathematical models of the immune response are increasingly recognized as powerful tools to gain understanding of complex systems. Several mathematical models have already been developed to describe antibody decay dynamics following vaccination or natural infection aiming at predicting long-term immunity. The more popular models are simple exponential decay models (e.g. Nommensen et al., 1989; Van Herck and Van Damme, 2001), bi-exponential decay models (e.g. Van Twillert et al., 2017; van Ravenhorst et al., 2016) or power-law decay models (e.g. Teunis et al., 2002). They are based on the assumption that antibody concentrations will decay over time. Changing slopes can be introduced to better fit immunological data, which typically show a higher antibody decay during the first period after immunization followed by a slower antibody decay.

ODE-systems are an extremely useful tool to model complex systems, because they are relatively easy to communicate, new biological assumptions can be included and several softwares exist to compute numerical solutions. To gain better insights on the dynamics of the humoral response, Le et al. (2015) proposed a model taking into account a population of specific ASCs and applied it to fit data from both ASCs and antibodies upon vaccinia virus immunization of human volunteers. This is the extension of a model developed by De Boer et al. (2001) and Antia et al. (2003) for modeling the CD8 T cell response. As stressed by the authors, this model may underestimate long-term immunity since it does not take into consideration antibody contribution supplied by long-lived ASCs (Halliley et al., 2015; Hammarlund et al., 2017).

The assumption of having several ASCs populations has been considered in several models thereafter. Fraser et al. (2007) considered an extension of the conventional power-law decay model to include two distinct populations of ASCs, differing in their respective decay rate, showing an improvement of data fitting. Andraud et al. (2012); White et al. (2014) developed models based on ordinary differential equations (ODEs) describing the contribution of short and long-lived ASCs in antibody production.

All previously cited models focus on the humoral response following immunization, without questioning the ability of the immune system to mount anamnestic responses. To the best of our knowledge, very few models have been proposed to address this question. An example is given by Wilson and Nokes (Wilson and Nokes, 1999; Wilson et al., 2007). The authors explored different mechanisms for the generation of immune memory and its role in enhancing a secondary response upon further immunization against hepatitis B virus. The memory compartment included

memory B and T cells and followed a logistic behavior. In this work, antibody and memory cell generation depended on the circulating antigen. The authors did not consider the contribution of any population of ASCs in generating and sustaining the antibody response. A memory B cell compartment, where memory B cells are supposed to follow a logistic behavior and could differentiate into ASCs, has been considered by Davis et al. (2018). The authors parametrized a model based on 12 ODEs of the humoral immune response against Shigella, a diarrheal bacteria, to describe the complex interactions of the bacteria with the host immune system. Nevertheless, the complexity of the proposed model entails several identifiability issues, making it difficult to be used in practice.

Pasin et al. (2019) have already analyzed the antibody response elicited by the two-dose heterologous vaccine regimens against Ebola virus based on Ad26.ZEBOV and MVA-BN-Filo, and evaluated during three phase I studies under the EBOVAC1 project. To this extent, they have used the model developed by Andraud et al. (2012). Model parameters have been estimated using a population approach and some key factors inducing variability in the humoral response have been identified and quantified. The model used by Pasin et al. focuses on the antibody response observed after the second dose, and can help predicting the durability of the antibody response following the two-dose heterologous regimens. However, the anamnestic response of any new exposure could not be studied, because no plasma cells nor memory B cells generation mechanism has been considered.

Here we want to extend the model developed by Andraud et al. (2012) to characterize the establishment of the humoral response after the first vaccine dose and its reactivation following the second dose. The generation of different subgroups of B cells -memory, short- and long-lived ASCs- is taken into account and a vaccine antigen compartment is considered as responsible for inducing the immune response. We aim at understanding the ability of vaccinated people to react to a potential future encounter with Ebola virus antigens. To this extent, we develop a model able to describe the generation of an anamnestic response by means of the establishment of the immunological memory.

Description of studies performed under the EBOVAC1 project and a descriptive analysis of antibody concentrations are given in Section 2. In Section 3 we formulate our mathematical model describing the humoral response to a single immunization and explain how it can be used to simulate further immunizations. In Section 4 we perform structural identifiability analysis to determine which data should be generated or alternatively which parameters should be fixed to allow proper parameter estimation. In Section 5 we perform a model calibration against available antibody concentration measurements. In Section 6, local sensitivity analysis completes previous results on parameter identifiability. With the parameter set obtained through calibration, in Section 7 we simulate a booster immunization which shows an improved immune response, due to the establishment of immunological memory elicited by the two-dose vaccination regimens. Finally in Section 8 we discuss the significance of obtained results and limitations of the model.

## 2. Study design and serological analyses

We consider data collected during three randomized, blinded, placebo-controlled phase I studies on healthy adult volunteers aged 18 to 50 years. Studies were performed in four different countries: UK, Kenya, Uganda and Tanzania. We present briefly these data here, because we will use them in next sections (e.g. Section 5). We refer to Milligan et al. (2016), Winslow et al. (2017), Mutua et al. (2019), and Anywaine et al. (2019) for a detailed pre-

**Table 1**

Summary of data analyzed per vaccination group.

| Group        | No. | Measurements                                 |
|--------------|-----|--|
| MVA/Ad26 D29 | 44  | D1, D8, D29, D36, D50, D180, D240, D360      |
| MVA/Ad26 D57 | 44  | D1, D8, D29, D57, D64, D78, D180, D240, D360 |
| Ad26/MVA D29 | 45  | D1, D8, D29, D36, D50, D180, D240, D360      |
| Ad26/MVA D57 | 44  | D1, D8, D29, D57, D64, D78, D180, D240, D360 |
| Total        | 177 |  |

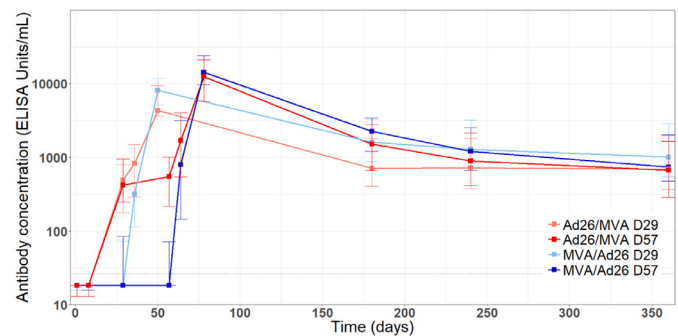


**Fig. 1.** Antibody concentrations dynamics per vaccination group in log<sub>10</sub> scale. (For interpretation of the references to colour in this figure legend, the reader is referred to the web version of this article.)

sensation of safety and immunogenicity results, for studies in UK, Kenya and Uganda/Tanzania respectively.

In each country, participants were randomized into four vaccination groups differing by the order of vaccine immunizations (Ad26.ZEBOV as first dose and MVA-BN-Filo as second dose or conversely) and by the interval of time between immunizations (either 28 or 56 days). Throughout the paper we will label vaccination groups specifying the order of vaccine immunizations and delay between the first and second doses, e.g. participants within group Ad26/MVA D57 have received the first Ad26.ZEBOV dose at day 1 and the second MVA-BN-Filo dose 56 days later. Vaccination group Ad26/MVA D57 will be considered as the reference group. In each study 18 volunteers were enrolled per vaccination group, 3 receiving placebo and 15 receiving active vaccine.

We have analyzed data from a total of 177 participants subdivided as described in Table 1. For all groups immunogenicity measurements have been recorded at the first immunization day (day 1), 7 days later (day 8), at the second immunization day (day 29 or 57), at both 7 days (day 36 or 64) and 21 days (day 50 or 78) after the second immunization, and at days 180, 240 and 360 after the first immunization for the follow-up. Groups receiving the second dose at day 57 have an extra immunogenicity measurement at day 29.

The humoral immune response to the vaccine has been assessed through analysis of IgG binding antibody concentrations against the Ebola virus Kikwit variant glycoprotein (EBOV GP). This was determined by enzyme-linked immunosorbent assay (ELISA) performed by Battelle Biomedical Research Center (BBRC, US) for the UK and Uganda/Tanzania studies and by Q2 Solutions (US) for the Kenya study with assay-specific limit of detection (LOD) varying among analyzing laboratory (36.6 ELISA units/mL for (BBRC), 26.22 ELISA units/mL for Q2 Solutions). Both laboratories used the same protocol and material for the assay.

In Fig. 1 the dynamics of antibody concentrations (median and interquartile ranges) per vaccination group is given, considering data from the three studies pooled together (for further details, see supplementary Figure S1 and supplementary Table S1).

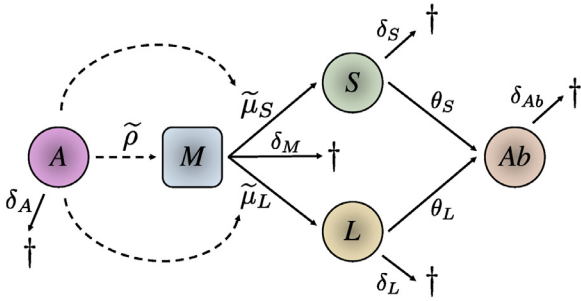


**Fig. 2.** Schematic representation of (MSL) model. A stands for vaccine antigen, M for memory B cells, S for short-lived ASCs, L for long-lived ASCs, and Ab for specific soluble antibodies. See text and Eqs. (1)–(5) for details.

### 3. Mathematical model for primary and anamnestic response

#### 3.1. Model formulation

To capture the establishment of the humoral immune response to a two-dose vaccination regimen and predict the reaction to a booster immunization, we propose a mathematical model based on a system of five ODEs (Eqs. (1)–(5)). We consider three B cell populations: memory B cells ( $M$ ), short-lived antibody secreting cells ( $S$ ) and long-lived antibody secreting cells ( $L$ ). In addition, we consider the concentration of antigen ( $A$ ), which is introduced through immunizations, and causes primary as well as secondary responses. Finally, antibody concentration ( $Ab$ ) is also described. For the sake of simplicity, we will denote this model as (MSL): a schematic representation is given in Fig. 2. Equations of our model are:

$$(MSL) = \begin{cases} \dot{A} = -\delta_A A & (1) \\ \dot{M} = \tilde{\rho} A - (\tilde{\mu}_S + \tilde{\mu}_L) A M - \delta_M M & (2) \\ \dot{S} = \tilde{\mu}_S A M - \delta_S S & (3) \\ \dot{L} = \tilde{\mu}_L A M - \delta_L L & (4) \\ \dot{Ab} = \theta_S S + \theta_L L - \delta_{Ab} Ab & (5) \end{cases}$$

The reaction is initiated when a certain amount of antigen  $A$  is detected by the host immune defenses at time  $t = 0$  (corresponding to the time of an immunization). The free antigen is progressively processed and eliminated from the system with the per capita rate  $\delta_A$  (Eq. (1)). The antigen dynamic is described by a simple exponential decay, because in this particular context neither of the two vaccine vectors are replicating (Milligan et al., 2016). The presence of antigen causes the instantaneous generation of  $M$  cells at rate  $\tilde{\rho} A$ , condensing the complex biological process of activation of specific naïve B cells, and their subsequent massive proliferation and maturation within GCs. The  $M$  compartment is then an “hybrid” one. While the reaction is ongoing,  $M$  cells differentiate into both short- and long-lived ASCs, at rates  $\tilde{\mu}_S$  and  $\tilde{\mu}_L$  respectively. After total antigen consumption,  $M$  denotes memory B cells (BMEMs), ready to differentiate into ASCs upon subsequent antigen stimulation. ASCs are ultimately differentiated cells which do not proliferate. They die with rate  $\delta_S$  and  $\delta_L$ , respectively. Antibodies are produced by both populations of ASCs in different proportions ( $\theta_S S + \theta_L L$ ). Their half-life is described by parameter  $\delta_{Ab}$ . Description of all parameters can be found in Table 2.

After some time, the reaction reaches a peak, then the production of new ASCs and BMEMs decreases and finally ends. Long-lived ASCs continue to produce antibodies assuring long-term immunity, while BMEMs persist in the organism to promote anamnestic responses in case of subsequent encounters with the same antigen. Indeed, in this case, BMEMs can differentiate into antigen-specific ASCs and produce high-affinity antibodies.

#### 3.2. Rescaled system

Compartment  $A$  is not observed in practice. In order to circumvent this difficulty, and to avoid identifiability issues (see Section 4), we can use the analytical solution of Eq. (1) in Eqs. (2) to (5). We get:

$$\begin{cases} \dot{M} = \rho e^{-\delta_A t} - (\mu_S + \mu_L) e^{-\delta_A t} M - \delta_M M \\ \dot{S} = \mu_S e^{-\delta_A t} M - \delta_S S \\ \dot{L} = \mu_L e^{-\delta_A t} M - \delta_L L \\ \dot{Ab} = \theta_S S + \theta_L L - \delta_{Ab} Ab \end{cases} \quad (6)$$

Note that through this transformation the unknown parameters are  $\rho := \tilde{\rho} A_0$ ,  $\mu_S := \tilde{\mu}_S A_0$ ,  $\mu_L := \tilde{\mu}_L A_0$  instead of  $\tilde{\rho}$ ,  $\tilde{\mu}_S$  and  $\tilde{\mu}_L$ , where  $A_0 := A(t = 0)$ .

#### 3.3. Special case: No memory cells death

It has been reported in the literature that BMEMs are an exceptionally stable population (Jones et al., 2015; Crotty et al., 2003). It is hence reasonable to assume that  $\delta_M \ll 1$ . Let us consider the rescaled system (6). Under the assumption  $\delta_M = 0$ , there exists a stationary state reached by BMEMs, given by:

$$M \stackrel{\delta_M=0}{=} \frac{\rho}{\mu_S + \mu_L} \quad (7)$$

The state (7) is globally asymptotically stable (Hartman and Olech, 1962). The assumption  $\delta_M \ll 1$  will be useful to interpret results in Sections 5 and 7. However, there is no constraint on this parameter in the sequel.

It is worth noting that in the case  $\delta_M > 0$ , the  $M$  population will converge exponentially towards 0. Nevertheless, provided that  $\delta_M \ll 1$  and in particular  $\delta_M \ll \delta_{Ab}$ , the decreasing slope of  $M$  will be very small, hence the effect of  $\delta_M$  will barely affect the  $Ab$  dynamics during the observation period.

#### 3.4. Special case: Absence of antigen stimulation

The model developed here extends a model proposed in Andraud et al. (2012) and applied in Pasin et al. (2019) in the context of the EBOVAC1 project to analyze the antibody response after the second dose. In these works the authors hypothesized that their observations began when the B cell response was already in the declining phase, i.e. there was no further generation of ASCs. In the absence of antigenic stimulus (e.g.  $A_0 = 0$ ), (6) reduces to:

$$\begin{cases} \dot{M} = -\delta_M M & (8) \\ \dot{S} = -\delta_S S & (9) \\ \dot{L} = -\delta_L L & (10) \\ \dot{Ab} = \theta_S S + \theta_L L - \delta_{Ab} Ab & (11) \end{cases}$$

This corresponds to the model used in Andraud et al. (2012) and Pasin et al. (2019), with the addition of Eq. (8) which does not affect Equations (9)–(11).

#### 3.5. Simulating the response to subsequent stimulations

The (MSL) model allows to describe the establishment of the humoral response by the first dose of antigen. To simulate the response to the second dose and subsequent stimulations, vaccine antigen is added to compartment  $A$  according to the vaccination schedule. Hence, the (MSL) model is applied again with predicted values of  $M$ ,  $S$ ,  $L$  and  $Ab$  the day of the planned second dose as new initial conditions. This can be mathematically formalized as follows.

Let  $n$  be the number of vaccine doses;  $t_i$ ,  $i = 1, \dots, n$  the time of administration of the  $i^{\text{th}}$ -dose and  $t_{n+1}$  the last observation time. Let  $\Psi := (\delta_{A,i}, \rho_i, \delta_{M,i}, \mu_{S,i}, \mu_{L,i}, \delta_{S,i}, \delta_{L,i}, \theta_{S,i}, \theta_{L,i}, \delta_{Ab,i})$  be the vector

**Table 2**

Description of model parameters with units. We represent by  $[A]$  the unit of antigen concentration: this quantity has not been measured in any study considered here.

| Parameter       | Description  | Unit  |
|-----------------|--|---|
| $\delta_A$      | Antigen declining rate   | days <sup>-1</sup>  |
| $\tilde{\rho}$  | Rate at which $M$ cells are generated over time per antigen concentration  | IgG-ASC.(10 <sup>6</sup> PBMC) <sup>-1</sup> .days <sup>-1</sup> . $[A]$ <sup>-1</sup>        |
| $\tilde{\mu}_S$ | Differentiation rate of $M$ cells into $S$ cells per antigen concentration | days <sup>-1</sup> . $[A]$ <sup>-1</sup>  |
| $\tilde{\mu}_L$ | Differentiation rate of $M$ cells into $L$ cells per antigen concentration | days <sup>-1</sup> . $[A]$ <sup>-1</sup>  |
| $\delta_M$      | Declining rate of $M$ cells  | days <sup>-1</sup>  |
| $\delta_S$      | Death rate of $S$ cells  | days <sup>-1</sup>  |
| $\delta_L$      | Death rate of $L$ cells  | days <sup>-1</sup>  |
| $\theta_S$      | Antibody production rate per $S$ cells                                     | ELISA Units.mL <sup>-1</sup> .(IgG-ASC) <sup>-1</sup> 10 <sup>6</sup> PBMC.days <sup>-1</sup> |
| $\theta_L$      | Antibody production rate per $L$ cells                                     | ELISA Units.mL <sup>-1</sup> .(IgG-ASC) <sup>-1</sup> 10 <sup>6</sup> PBMC.days <sup>-1</sup> |
| $\delta_{Ab}$   | Antibody death rate  | days <sup>-1</sup>  |

of unknown parameters associated with the immune response to the  $i^{\text{th}}$ -dose. We denote the initial conditions by  $M_0, S_0, L_0, Ab_0$ .

For  $t_i < t \leq t_{i+1}$ ,  $i = 1, \dots, n$ , the dynamics of  $M, S, L, Ab$  following the  $i^{\text{th}}$ -immunization is obtained as the solution to the following ODE system:

$$\begin{cases} \dot{M} = \rho_i e^{-\delta_{A,i}(t-t_i)} - (\mu_{S,i} + \mu_{L,i}) e^{-\delta_{A,i}(t-t_i)} M - \delta_{M,i} M \\ \dot{S} = \mu_{S,i} e^{-\delta_{A,i}(t-t_i)} M - \delta_{S,i} S \\ \dot{L} = \mu_{L,i} e^{-\delta_{A,i}(t-t_i)} M - \delta_{L,i} L \\ \dot{Ab} = \theta_{S,i} S + \theta_{L,i} L - \delta_{Ab,i} Ab \end{cases}, \quad (12)$$

with initial conditions:  $M_0 = M(t = t_i), \dots, Ab_0 = Ab(t = t_i)$ .

#### 4. Identifiability analysis

We have performed a theoretical study of the rescaled model described by (6) to determine which biological data are needed to accurately estimate parameters and infer predictions about two-dose vaccination regimens.

*A priori* structural identifiability is a structural property of a model. It ensures a sufficient condition for recovering uniquely unknown model parameters from knowledge of the input-output behavior of the system under ideal conditions (*i.e.* noise-free observations and error-free model structure). We refer to Miao et al. (2011) for a formal definition of *a priori* structural identifiability.

Ideally one would assess global structural identifiability, but sometimes local identifiability can be sufficient if *a priori* knowledge on the unknown parameters allows to reject alternative parameter sets. For instance, global identifiability for (6) would not be reached without imposing any condition on the half-life of compartment  $S$  compared to  $L$ . Indeed, from a structural point of view, the roles of  $S$  and  $L$  are perfectly symmetric.

We assess local structural identifiability of (6) using the IdentifiabilityAnalysis package implemented in Mathematica (Appendix A). We suppose that  $Ab_0 = Ab(t = 0)$  is known and  $Ab(t)$  is observed during follow-up, which is consistent with available data (Section 2). If all other initial conditions are unknown, (6) results in being non-identifiable (Supplementary Table S2). The non-identifiable parameters are  $L_0, M_0, S_0, \mu_L, \mu_S, \rho, \theta_L, \theta_S$ , with degree of freedom 2. This means that, in order to solve the non-identifiability issue, one should fix at least two parameters within the set of non-identifiable parameters,  $\{\mu_L, \mu_S, \rho, \theta_L, \theta_S\}$ . However, there is no available information on the values of these parameters, hence they cannot be fixed *a priori*. Therefore, additional biological data corresponding to other compartments need to be integrated to ensure structural identifiability.

Analyses of specific B cell responses induced by vaccination could be performed through the Enzyme-Linked Immunosorbent Spot Assay (ELISpot). This is a sensitive method to identify the concentration of antigen-specific ASCs (Shah and Koelsch, 2015). Antigen-specific BMEMs can also be analyzed through the ELISpot

techniques, but this requires *ex vivo* polyclonal activation over 3 to 8 days before detectable amounts of antibodies can be found.

Specific ASCs correspond in (6) to  $(S + L)(t)$ . Let us assume they are measured during follow-up; baseline values of both  $S$  and  $L$  are still supposed unknown. We obtain that Model (6) with unknown parameter vector  $\psi := (\delta_A, \rho, \mu_S, \mu_L, \delta_M, \delta_S, \delta_L, \theta_S, \theta_L, \delta_{Ab})$ , and outputs vector  $y(t) = (Ab_0, Ab(t), (S + L)(t))$  is *a priori* structurally identifiable (Supplementary Table S2).

Let us assume that the  $M$  compartment is observed during follow-up instead of  $S + L$ . In this case, the structural identifiability of Model (6) is not ensured, according to the IdentifiabilityAnalysis algorithm (Supplementary Table S2). Other parameters should be fixed or information about ASCs should be integrated.

We can conclude that  $\{Ab_0, Ab(t), (S + L)(t)\}$  is a suitable minimal output set to be considered to ensure model identifiability. Of course any other additional information about parameters and/or model compartments will increase the identifiability of (6) and the reliability of parameter estimation.

Of note, this analysis of theoretical identifiability still does not guarantee practical identifiability, which depends on availability and quality of data (Miao et al., 2011), such as time point distribution of measurements and measurements errors. However, practical identifiability could be improved by using a population approach for parameter estimation based on mixed-effects models (Lavielle and Aarons, 2016; Guedj et al., 2007; Prague et al., 2013). This approach allows to perform parameter estimation across a whole population of individuals simultaneously, and quantify the variations that some covariates (either categorical and continuous) of interest produce over the dynamics of specific subgroups (*e.g.* heterogeneous vaccination schedules). This is done by assuming some underlying structure to the distribution of individual-level parameters across a population. Firstly, each individual parameter is described by an intercept representing the mean parameter value across the whole population. Then, part of variability can be described by way of covariates allowing the distinction between different sub-populations, and finally a normally distributed random effect characterizes the remaining between-subjects unexplained variability. Within this framework, either maximum likelihood and Bayesian approaches have been proposed to perform parameter estimation.

#### 5. Model calibration

Model (6) is not structurally identifiable with the observation of compartment  $Ab$  only: a reliable parameter estimation cannot be performed. Therefore, we propose a model calibration against antibody concentration data to assess the ability of (6) to reproduce antibody kinetics consistent with available experimental data.

**Table 3**

Let  $\psi$  be a generic (unknown) parameter in  $\{\delta_A, \rho, \mu_S, \mu_L, \delta_M, \delta_S, \delta_L, \theta_S, \theta_L, \delta_{Ab}\}$ . If it is dependent on the interval between immunizations or vaccine vector we write  $\psi(\text{cat})$ , “cat” being a possible category of each variability factor.

| $\psi(\text{cat})$    |          |                                   |
|-----------------------|----------|-----------------------------------|
| Factor                | Category | Meaning                           |
| <b>Timing</b>         | PVD1     | Post vaccination at day 1         |
|                       | PVD29    | Post second vaccination at day 29 |
|                       | PVD57    | Post second vaccination at day 57 |
| <b>Vaccine vector</b> | MVA      | The vaccine vector is MVA-BN-Filo |
|                       | Ad26     | The vaccine vector is Ad26.ZEBOV  |

### 5.1. Methods

To perform the calibration, we considered the antibody concentration data as described in Section 2.

We calibrated (6) considering the median and interquartile ranges among all studies pooled together stratified by vaccination group, considering vaccination group Ad26/MVA D57 as the reference group.

$M(0)$ ,  $S(0)$ ,  $L(0)$  and  $Ab(0)$  were set equal to 0 before the first dose, i.e. we supposed there were no previously existing specific antibodies nor B cells. Initial conditions of the reaction to the second dose are set as the predicted values of each compartment at the second dose immunization day, as described in Section 3.5. Simulations of (6) have been performed using Matlab, ode45 function. According to biological assumptions or previous modeling results, we suppose that the following parameters could be modified depending on the vaccine vector and/or the timing of dose administration (see Table 3 for notation details):

- $\rho$ ,  $\mu_S$ ,  $\mu_L$  are vector dependent (Ad26.ZEBOV or MVA-BN-Filo). These parameters determine the strength of the humoral response and the amount of ASCs and BMEMs generated (Section 3). Biological evidences suggest that the strength and quality of the immune response is dependent on the type of antigen inducing the reaction and the way it is presented (e.g. Sallusto et al., 2010).
- $\delta_S(\text{PVD1}) \geq \delta_S(\text{PVD29}) \geq \delta_S(\text{PVD57})$ : Pasin et al. (2019) have identified a significant effect of the delay between immunizations on  $\delta_S$  by analyzing the same phase I data we are considering here, with a simplified mechanistic model.

- $\delta_S(\text{Ad26}) \neq \delta_S(\text{MVA})$ : the effect of the order of administration of vaccine vector over the decay rate of short-lived ASCs has been evidenced in a previous analysis by Pasin et al. (2019). The higher complexity of the model described here allows to define a direct dependence between parameters and vaccine vectors: we allow parameter  $\delta_S$  to change according to the vaccine vector used.
- $\rho(\text{PVD1}) < \rho(\text{PVD29}) \leq \rho(\text{PVD57})$ : the secondary response is improved in magnitude with respect to the primary one, due to the presence of specific BMEMs contributing to the initiation of GCs reaction in a more effective way (Tangye et al., 2003). Parameter  $\rho$  determines the strength of the humoral response because it defines the generation of  $M$  cells upon antigen stimulation, i.e. the GC reaction breadth. Therefore  $M$  cells do not play exactly the same role when a primary (GCs generated from activated naïve B cells) or a secondary (GCs seeded by BMEMs or newly activated naïve B cells; BMEMs differentiating into ASCs) response is simulated (Inoue et al., 2018; Ademokun and Dunn-Walters, 2010), hence it is reasonable to allow parameter  $\rho$  to increase from the first immunization ( $\rho(\text{PVD1})$ ) to the following one ( $\rho(\text{PVD29})$  or  $\rho(\text{PVD57})$ ). In addition, previous studies on different viruses and vaccines have shown that an increased interval between immunizations is associated with an improved magnitude of the response (e.g. Jilg et al., 1989; Belshe et al., 2011). Consequently, an additional variation of parameter  $\rho$  depending on the interval between the two doses is permitted.
- $\delta_A(\text{Ad26}) \leq \delta_A(\text{MVA})$ : according to biodistribution and persistence results, Ad26 is cleared in approximately 3 months (Sheets et al., 2008), while MVA is cleared in approximately 1 month (Hanke et al., 2005). Note that here antigen concentration defines the duration of the GC response, so it does not exactly reflect biodistribution.

Model calibration has been achieved by repeated simulations of (6) and parameter tuning, until we obtained a consistent parameter set able to reproduce reasonable antibody dynamics in accordance with interquartile ranges of experimental data for all vaccination groups.

### 5.2. Results

Table 4 shows parameter values obtained at the end of the calibration process described in Section 5.1.

In Fig. 3, antibodies (Fig. 3 (a)) and ASCs and BMEMs (Fig. 3 (b)) dynamics are plotted for the reference vaccination group,

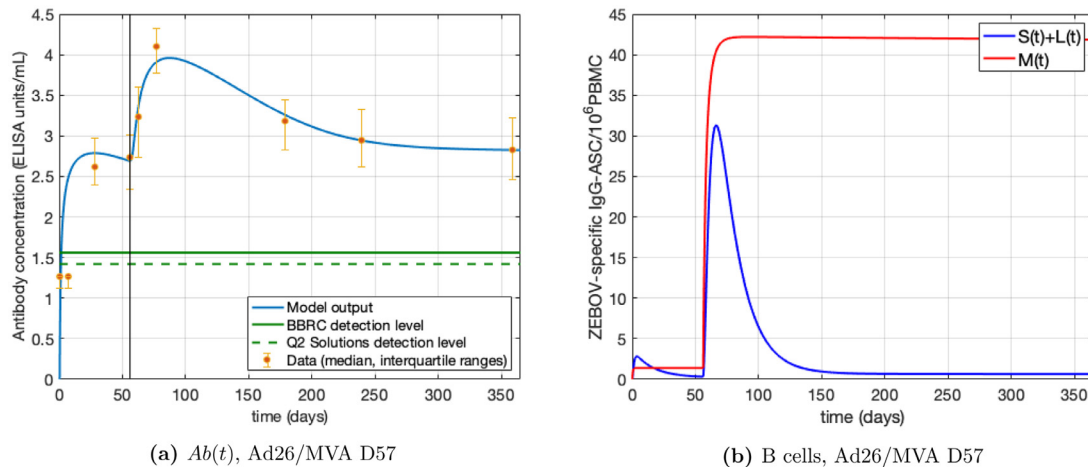


**Fig. 3.** Predictions from the calibrated (MSL) model for the reference group, Ad26/MVA D57. (a) Antibody concentrations ( $\log_{10}$ -transformed). Green horizontal lines denote detection levels used by the BBRC laboratory (solid line) and by the Q2 Solutions laboratory (dashed line) respectively. (b) B cells,  $S$  and  $L$  stand for short-lived and long-lived ASCs respectively;  $M$  represents BMEMs.

**Table 4**

Parameters set obtained through (MSL) model calibration and used for simulations plotted in Fig. 3 and supplementary Figures S2-S3. The half-life corresponding to rate loss parameters is given by:  $t_{1/2}(\delta_i) := \ln(2)/\delta_i$ . Structurally identifiability of parameters with antibody concentrations observations is recalled, according to results of Section 4 (Y=structurally identifiable; N=structurally non-identifiable).

| Parameter              | Prior     | Ref.                 |                        | Value           |                 | Unit  | Structurally identifiable with measured Ab only? |
|------------------------|-----------|----------------------|------------------------|-----------------|-----------------|---|--|
|                        |           |                      |                        | Ad26            | MVA             |   |  |
| $t_{1/2}(\delta_A)$    | -         | -                    |                        | 10.7            | 3.3             | days (half-life is derived from the approximate time to clear Ad26.ZEBOV and MVA-BN-Filo respectively : $t_{1/2}(\delta_A)(\text{Ad26}) > t_{1/2}(\delta_A)(\text{MVA})$ Sheets et al. (2008); Hanke et al. (2005)) | Y  |
| $\rho$                 | -         |                      | PVD1<br>PVD29<br>PVD57 | 3.5<br>15<br>15 | 0.7<br>17<br>20 | IgG-ASC/ $10^6$ PBMC.days $^{-1}$   | N  |
| $\mu_S$                | -         |                      |                        | 2.5             | 0.4             | days $^{-1}$  | N  |
| $\mu_L$                | -         |                      |                        | 0.011           | 0.0035          | days $^{-1}$  | N  |
| $t_{1/2}(\delta_M)$    | $\geq 50$ | Crotty et al. (2003) |                        | 63.3            |                 | years   | Y  |
| $t_{1/2}(\delta_S)$    | -         |                      | PVD1<br>PVD29          | 0.7<br>2.8      | 0.7<br>4.6      | days  | Y  |
|                        | [0.8;7.7] | Pasin et al. (2019)  | PVD57                  | 4.6             | 11.6            |   |  |
| $t_{1/2}(\delta_L)$    | [2.7;13]  | Pasin et al. (2019)  |                        | 9.5             |                 | years   | Y  |
| $\theta_S$             | -         |                      |                        | 20              |                 | ELISA   | N  |
|                        |           |                      |                        |                 |                 | Units/mL.(IgG-ASC/ $10^6$ PBMC) $^{-1}$ .days $^{-1}$   |  |
| $\theta_L$             | -         |                      |                        | 30              |                 | ELISA   | N  |
|                        |           |                      |                        |                 |                 | Units/mL.(IgG-ASC/ $10^6$ PBMC) $^{-1}$ .days $^{-1}$   |  |
| $t_{1/2}(\delta_{Ab})$ | [22;26]   | Pasin et al. (2019)  |                        | 23.9            |                 | days  | Y  |

Ad26/MVA D57, as an example. Results for all other vaccination groups are given in supplementary Figures S2-S3. The time axis is rescaled at the day of the primary injection (i.e. study day 1) and simulations performed up to 1 year after the first dose.

In Fig. 3 (a), orange dots correspond to median values of antibody concentrations data from the corresponding vaccination group. We were able to satisfactorily reproduce antibody concentrations dynamics in accordance with experimental observations for all vaccination groups. In supplementary Table S3 further details are given, with comparison of simulations to real data at some point of interest, e.g. at the time of the observed antibody peak and one year after the first dose.

The model predicts that antibody levels at one year after the first dose are comparable among all vaccine regimens, in accordance with data. The antibody response peak has been measured 21 days after the second dose. Antibody dynamics obtained with our calibration show a slightly delayed peak between 3 and 4 weeks after the second dose. Of note, no immunogenicity measurements have been performed e.g. at 2 weeks nor at 4 weeks.

In Fig. 3 (b) the dynamics of B cells are plotted: for ASCs, we consider the sum of short- and long-lived ASCs. Note that, because the half-life of short-lived B cells is supposed to be significantly shorter than long-lived B cells one, at 1 year of follow-up we do not have any contribution from the S compartment.

Results about B cell subsets dynamics correspond only to model predictions since they were not calibrated on real data, therefore model parameters could not be accurately determined. However, with the data available so far from phase I studies, this model provides a good starting point and it will be further implemented and validated when additional biological data on B-cells populations from ongoing phase II and phase III clinical studies will be available. ASCs dynamic shows an early peak located a few days (between 7 to 10) after the second dose. This is in accordance with other studies assessing B cell kinetics upon vaccination (e.g. Halliley et al., 2010; Leach et al., 2013). It is followed by a rapid relaxation phase, then stabilization.

The rapid decreasing slope after the peak of the ASCs response (i.e. from approximatively 1 to 10 weeks after the second dose) de-

pends on the value of parameter  $\delta_S$ , which corresponds to a very small half-life of short-lived ASCs (varying from almost 3 to 12 days, depending on the regimen). The concentration of long-lived ASCs is low for the obtained parameter set, but able to sustain the antibody response due to the long half-life of this population. BMEM level depends on parameters  $\rho$ ,  $\mu_S$  and  $\mu_L$ , as stressed in Section 3.3 (note that according to Table 4 the half-life of M cells is set here at about 63 years, which implies a really weak value for parameter  $\delta_M$ , of the order of  $10^{-5}$ ).

## 6. Sensitivity analysis of the antibody compartment

We have obtained a parameter set able to reproduce antibody responses dynamics to two-dose vaccine regimens against Ebola virus that closely resemble experimental observations. We perform a local sensitivity analysis of the antibody compartment to clarify the effect of each parameter on it over time. This can help detecting two different sources of practical non-identifiability of parameters:

1. a very weak effect of a given parameter on the observed compartment or an effect which is concentrated in a specific time window where observations are very scarce;
2. the interplay among parameters: the effect of the variation of one parameter on the observed compartment can be compensated by a suitable variation of another parameter.

An intuitive representation of local sensitivity of the Ab compartment with respect to each parameter is given by the evaluation of curves  $\phi_{\psi_i}(t) := \frac{\psi_i}{Ab(t, \psi)} \frac{\partial Ab(t, \psi)}{\partial \psi_i} \Big|_{\psi=\psi^*}$ , for each parameter  $\psi_i$  in  $\psi = \{\delta_A, \rho, \delta_M, \mu_S, \mu_L, \delta_S, \delta_L, \theta_S, \theta_L, \delta_{Ab}\}$  (Zi, 2011). The quotient  $\psi_i/Ab$  is introduced to normalize the coefficient and avoid influence of units.

### 6.1. Results

Partial derivatives of (6) Ab output with respect to each parameter are numerically evaluated (Appendix B).  $\psi^*$  is set at parameter values corresponding to the reference regimen, Ad26/MVA D57

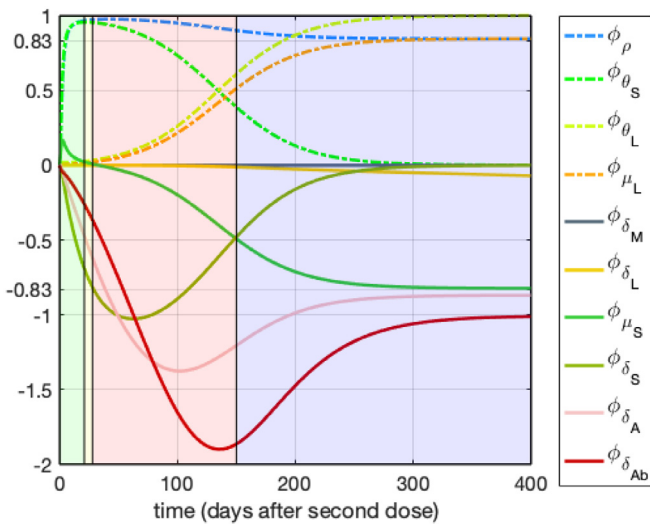


**Fig. 4.** Relative sensitivity of the Ab compartment with respect to (MSL) parameters over time. For each parameter  $\psi_i$  in  $\psi = \{\rho, \theta_S, \delta_S, \delta_A, \delta_{Ab}, \theta_L, \mu_S, \mu_L, \delta_M, \delta_L\}$  the normalized sensitivity coefficients are plotted:  $\phi_{\psi_i}(t) := \frac{\psi_i}{Ab(t, \psi)} \frac{\partial Ab(t, \psi)}{\partial \psi_i}$ . For the sake of clarity we shaded differently time windows corresponding to distinct phases of the antibody kinetics: in green the first exponential phase, in yellow the antibody peak, in pink the declining phase, in blue the stabilization phase. (For interpretation of the references to colour in this figure legend, the reader is referred to the web version of this article.)

(Table 4). In Fig. 4,  $\phi_{\psi_i}(t)$  for all  $\psi_i$  in  $\psi$  are plotted. The time axis is rescaled at the day of the second dose administration.

The influence of almost all parameters over Ab dynamics significantly changes over time. In particular, in the very early exponential phase after vaccine immunization, parameters that mostly influence the antibody response in (6) are  $\rho$ , which determines the intensity of the immune response upon antigen stimulation, and  $\theta_S$  and  $\delta_S$ , characterizing the antibody production rate of short-lived ASCs and their half-life respectively. Right after the antibody peak, the most relevant parameters are the decay rate of antigen  $\delta_A$  and the half-life of antibodies  $\delta_{Ab}$ . Asymptotically, we will mostly retain the influence of  $\delta_{Ab}$  and the antibody production rate of long-lived ASCs  $\theta_L$  (even if  $\delta_A$ ,  $\rho$ , and the differentiation rates of M cells into both compartments of ASCs,  $\mu_S$  and  $\mu_L$ , also have a great influence).

From curves plotted in Fig. 4 it is also possible to deduce in which direction each parameter affects the Ab dynamics: increasing the values of  $\rho$ ,  $\mu_L$ ,  $\theta_S$  and  $\theta_L$  implies an increase in Ab concentration. The loss rates  $\delta_A$ ,  $\delta_S$ ,  $\delta_{Ab}$ ,  $\delta_L$  and parameter  $\mu_S$  (starting from a few weeks post vaccination) acts in the opposite way: an increase of their values is associated to a decrease of the Ab concentration. Note that the sensitivity of Ab with respect to  $\mu_S$  is positive during the first weeks after vaccination, because this parameter determines the generation of short-lived ASCs, which govern the early antibody response.

The half-lives of both M and L populations are supposed to be significantly greater than antibody half-life. This explains why parameters  $\delta_M$  and  $\delta_L$  have an extremely low influence over Ab dynamics on the one-year period considered and locally around parameter set given in Table 4. The reliability of their estimations could be refined either by considering longer follow-up or by integrating data related to these compartments (cf. specific BMEMs and ASCs through the ELISpot technique).

Finally, Fig. 4 shows that in absolute value, the sensitivity of Ab with respect to some parameters seems to asymptotically stabilize at the same value (starting from approximately 250 days after the second dose). We are referring to e.g. ( $\rho$ ,  $\mu_L$ ) in the same way, and

( $\delta_{Ab}$ ,  $\theta_L$ ) in opposite ways. This has consequences on the identifiability of these parameters: the effect of the variation of one among them can be compensated by a suitable variation of its pair, at least over some specific time windows. This implies that if antibody observations are collected exclusively within these time windows, it would not be possible to accurately estimate these parameters individually, due to their interplay.

A particular focus should be made on parameters  $\mu_S$  and  $\mu_L$ : the sensitivity of Ab with respect to these parameters is symmetric (in opposite way) over time starting early (few weeks) after immunization. Henceforth the Ab dynamics will be unchanged by preserving the quotient between  $\mu_S$  and  $\mu_L$  (note that (6) is not identifiable if the only observed compartment is Ab). In Fig. 5 (a) we plot the Ab dynamics obtained when both  $\mu_S$  and  $\mu_L$  are increased by 50% simultaneously: we can see that the obtained curves are superposed. Nevertheless, the corresponding M dynamics is significantly affected by changes in the individual values of  $\mu_S$  and  $\mu_L$ , as shown in Fig. 5 (b). This further stress the importance of integrating further biological data to proceed to parameter estimation in a reliable manner.

## 6.2. Conclusions

Sensitivity analysis is used to gain a better understanding of the practical identifiability of model parameters from antibody concentrations data.

The sensitivity of antibody dynamics with respect to parameters  $\delta_M$  and  $\delta_L$  is extremely weak: changing their values does not affect significantly the Ab output, at least in the considered time window. We conclude that these parameters are practically non-identifiable considering only antibody data and one year of follow-up.

Parameters  $\mu_S$  and  $\mu_L$  are closely related, affecting antibody dynamics in a symmetric way. Antibody concentration data would not allow their estimation individually, due to their collinearity.

Other parameters will be practically non-identifiable due to data quality (e.g. time point distribution and/or measurements errors and limitations). In particular, one should pay particular attention to parameters which exclusively describe the reaction to the first vaccine dose. Indeed, very few antibody measurements are above the detection level before the second dose, in particular for patients primed with MVA-BN-Filo (Section 2).

## 7. Simulations of a booster dose

One of the main interests in modeling the establishment and reactivation of the immune response after multiple antigen exposures is the prediction of the effects of a booster dose. With (6) we can expect to be able to predict the strength of an anamnestic response by the mean of the establishment of an effective immunological memory.

We use the calibrated model (6) to simulate the response to an Ad26.ZEBOV booster dose, realized at day 360 after the first dose for vaccination group Ad26/MVA D57.

In order to simulate the first two immunizations (i.e. the regular two-dose schedule), we use the parameter set obtained in Section 5 (Table 4). The Ad26.ZEBOV booster dose is simulated using the parameter set corresponding to an Ad26.ZEBOV immunization 56 days after the first dose.

In Fig. 6 we plot the dynamics of both antibodies ( $\log_{10}$ -transformed) and B cells (ASCs and BMEMs) as predicted by (6) for the second dose and booster immunizations. The time axis is rescaled to have time 0 corresponding to the second immunization day (i.e. day 57). Further information is given in supplementary Table S4.

Simulations show a strong humoral anamnestic response to the booster immunization, with approximately a 11-fold increase of

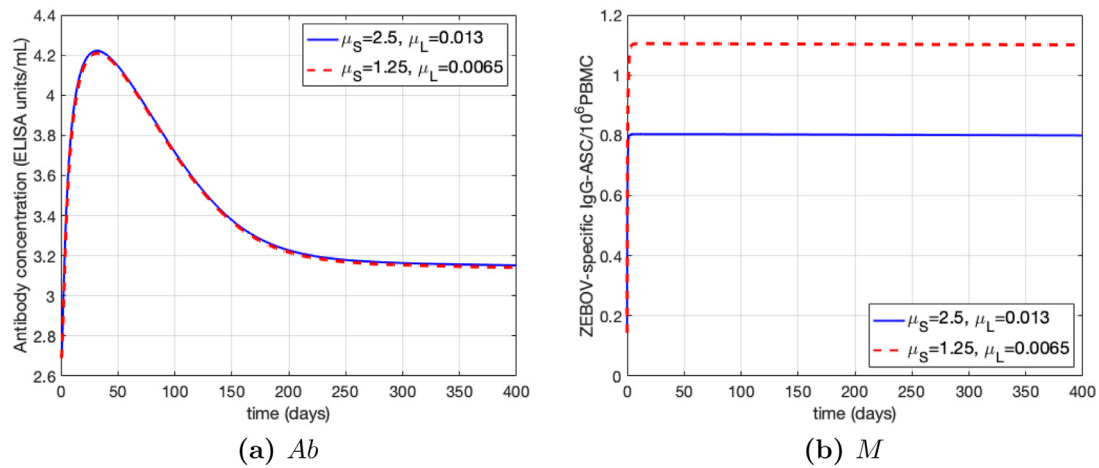


**Fig. 5.** Effects of a variation of both  $\mu_S$  and  $\mu_L$  of 50% on (a)  $Ab$  and (b)  $M$  (all other parameters are fixed as in Table 4).

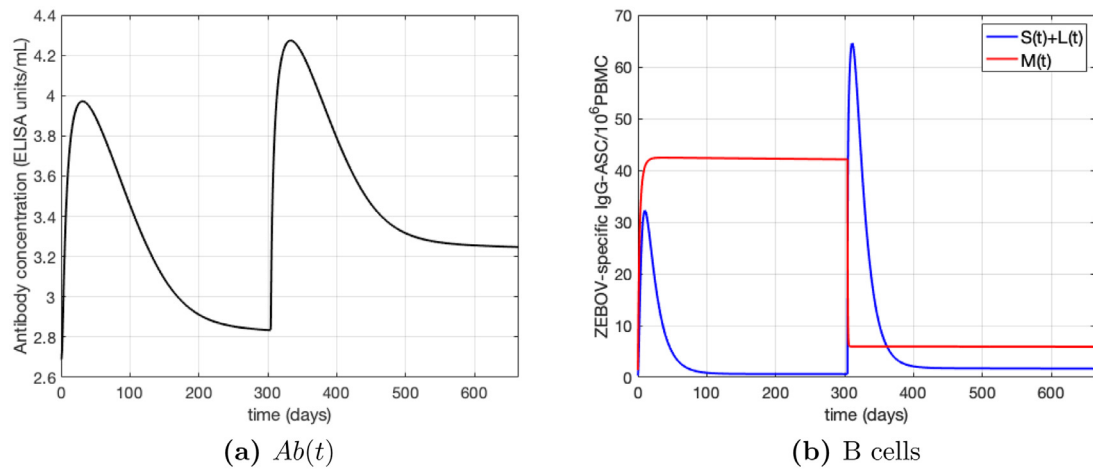


**Fig. 6.** Simulation of (MSL) for vaccination group Ad26/MVA D57 with a booster dose of Ad26.ZEBOV one year after the first dose (day 360). In (a) the obtained  $\log_{10}$ -transformed antibody concentration is given. In (b)  $S$  and  $L$  stand for short-lived and long-lived ASCs respectively;  $M$  represents memory cells. The time axis is rescaled at the second dose day (i.e. day 57).

antibody concentration within 7 days post booster dose, and a 25-fold increase within 21 days (in linear scale). This is due to the presence of a high affinity pool of BMEMs which differentiate into ASCs directly upon antigen stimulation. In addition, the model predicts a 2.5-fold increase in antibody concentration 360 days after the booster dose (i.e. day 720) compared to day 360.

In Fig. 6 (b) we have plotted the corresponding B cell dynamics. Again, we observe that ASCs increase drastically after the booster immunization, hence stabilizes at a higher level than before, correlating with antibody concentrations. After the booster dose, BMEMs stabilize at a lower level: this depends on the calibrated values for parameters  $\rho$ ,  $\mu_S$  and  $\mu_L$  under the assumption that the effect of Ad26.ZEBOV as booster dose would be similar to Ad26.ZEBOV at Day 57 as second dose. We anticipate that, from an immunological perspective, depletion of BMEM (Fig. 6 (b)) is not reflecting the immunological situation post booster dose, because replenishment of the BMEM compartment is to be expected after booster vaccination. Otherwise, this would mean that after a few encounters with the same antigen, instead of building up stronger immunity and memory like what is observed in real life for many pathogens (Li et al., 2012; Lessler et al., 2012; Green et al., 2018), the memory would have a lower level. With these regards, we ran additional sensitivity analyses in which we decreased the values

of the parameters  $\mu_S$  and  $\mu_L$  for the booster dose of Ad26.ZEBOV down to 10-fold lower values (Fig. 7). We show that, by modifying these values the BMEMs (Fig. 7 (a)) reach higher levels, while both the antibody levels (Fig. 7 (b)) and the plasma cells levels (Fig. 7 (c)) are similar for the different sets of parameters ( $\mu_S$ ,  $\mu_L$ ). Immunologically, the variation of parameters  $\mu_S$  and  $\mu_L$  for the booster dose can be justified by assuming a complete maturation (hence effectiveness upon antigen stimulation) of the BMEMs only at the time of the booster (and not at dose 1/dose 2) (Jilg et al., 1989; Belshe et al., 2011).

If experimentally confirmed, these results would suggest the establishment of an effective immunological memory against Ebola virus, as a response to the two-dose vaccine regimen. Model predictions about the effects of a booster dose could be further evaluated when supplementary immunological data from a subgroup of ongoing phase II clinical studies which received booster dose of Ad26.ZEBOV will be available (Ebovac2, 2018).

## 8. Discussion

Recurring Ebola outbreaks have been recorded in equatorial Africa since the discovery of Ebola virus in 1976, with the largest and more complex one occurred in West Africa between March

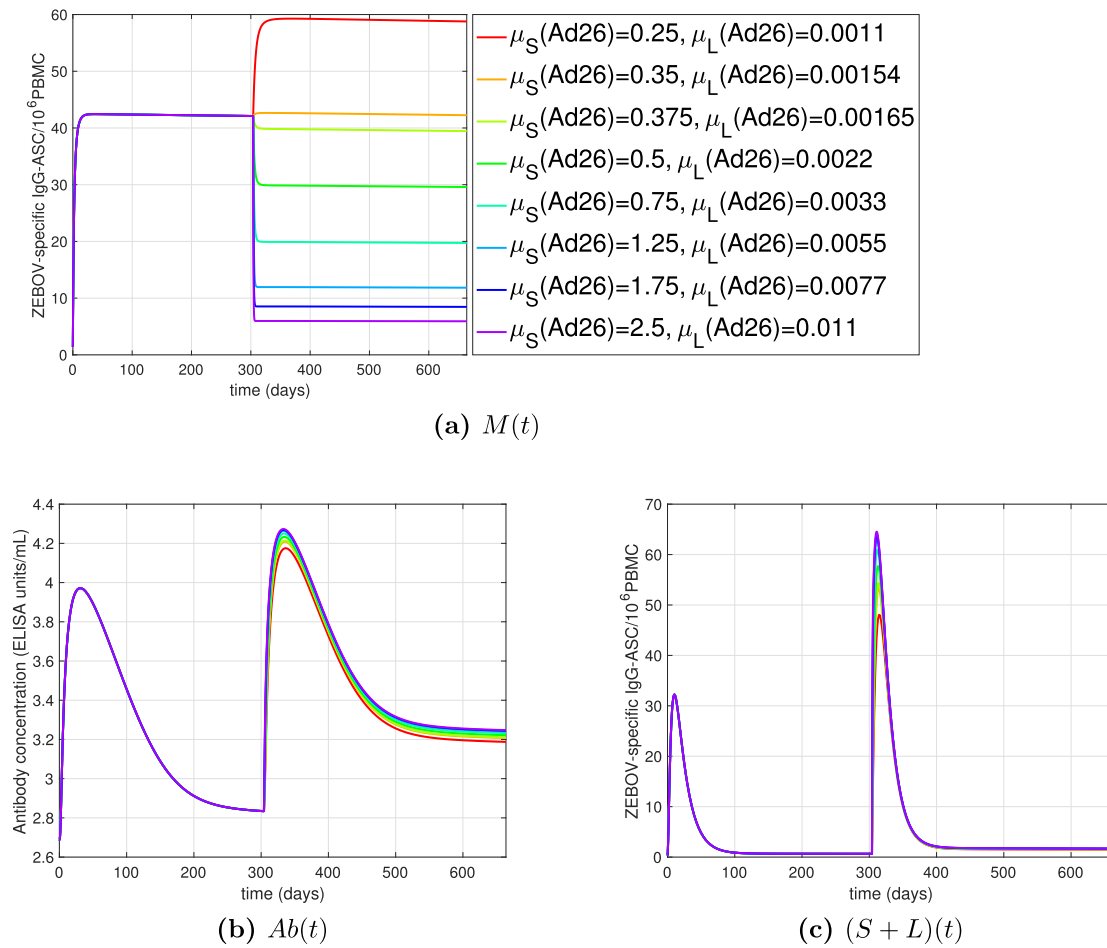


**Fig. 7.** Simulation of (MSL) for vaccination group Ad26/MVA D57 with a booster dose of Ad26.ZEBOV one year after the first dose (day 360), when both  $\mu_S(\text{Ad26})$  and  $\mu_L(\text{Ad26})$  for the booster dose of Ad26.ZEBOV are varied by (from top to bottom, see legend in (a)) 90%, 86%, 85%, 80%, 70%, 50%, 30% from the reference value as in Table 4 (purple curve). In (a) the corresponding  $M$  dynamics are given, in (b) the  $\log_{10}$ -transformed antibody concentration and in (c) the ASCs dynamics. The time axis is rescaled at the second dose day (i.e. day 57). (For interpretation of the references to colour in this figure legend, the reader is referred to the web version of this article.)

2014 and June 2016. We are now currently experiencing, in the DRC, the second largest outbreak ever recorded. A prophylactic vaccine against Ebola virus is urgently needed.

A new two-dose heterologous vaccine regimen against Ebola Virus based on Ad26.ZEBOV and MVA-BN-Filo developed by Janssen Vaccines & Prevention B.V. in collaboration with Bavarian Nordic is being evaluated in multiple clinical studies. The immune response following vaccination has been mainly assessed through specific binding antibody concentrations (Section 2). The level of circulating antibodies needed to ensure protection is currently unclear: persistence of antibody responses after the two-dose vaccination has been clinically observed up to one year after the first dose, yet at a lower level than shortly after vaccination. Since we don't currently know for how long the two-dose vaccine can convey protection, a booster vaccination can be considered in case of imminent risk of exposure to Ebola virus (pre-exposure booster vaccination).

We proposed an original mechanistic ODE-based model - (MSL) - which takes into account the immunological memory (BMEMs) and short- and long-lived ASCs dynamics (Section 3). This model, which is an extension of the model developed by Andraud et al. (2012), aimed at explaining the primary response after receiving a first vaccine dose against Ebola virus, and the secondary response following a second heterologous vaccine dose. The final goal of our model is to predict the speed and magnitude of

the anamnestic response triggered by a booster vaccination among individuals who have been vaccinated with the two-dose regimen, and the long-term antibody persistence afterward. Succeeding in this task will be extremely helpful to better understand the immune response to a vaccine regimen.

We have performed structural identifiability analysis of (MSL) model (Section 4), which pointed out that antibody concentrations data are not sufficient to ensure (MSL) structural identifiability. Indeed, different parameter sets can reproduce the same antibody dynamic. In order to proceed with proper parameter estimation, at least ASCs data should be integrated. Alternatively, some parameters should be fixed to allow estimation of the remaining ones.

In the absence of priors on structural non-identifiable parameters and of additional biological data, we decided to proceed to model calibration (Section 5). To perform (MSL) model calibration, we have repeatedly simulated (MSL) using Matlab and compared the  $Ab$  output to median and interquartile ranges of available ELISA data from all studies pooled together, stratified by vaccination group. We have shown that (MSL) model is able to reproduce qualitatively the observed antibody kinetics for a well-chosen set of parameters. This provides the rationale to test the ability of (MSL) in predicting the speed and magnitude of the immune response to a booster vaccine dose.

Based on parameter values obtained through (MSL) model calibration, we have performed local sensitivity analysis to assess

to which extent each parameter affects antibody dynamics over time (Section 6). Hence, a better insight on practical identifiability of model parameters has been achieved in a sensitivity-based manner.

Finally, the calibrated model has been used to evaluate *in silico* a booster dose of Ad26.ZEBOV one year after the first dose (Section 7), showing a strong humoral anamnestic response. If experimentally confirmed, this would increase confidence on the capacity of the proposed prophylactic regimen to induce a robust and durable immune response against Ebola virus.

In order to simplify the model structure, in (MSL) the  $M$  compartment describes the GC reaction and the contribution of the BMEM population to the immune response. Therefore, due to the intrinsic difference between the primary and the secondary responses,  $M$  cells do not play exactly the same role when a primary (GCs generated from activated naïve B cells) or a secondary (GCs seeded by BMEMs or newly activated naïve B cells; BMEMs differentiating into ASCs) response is simulated (Inoue et al., 2018; Ademokun and Dunn-Walters, 2010). For this reason, it is reasonable to adjust some parameters (e.g.  $\rho$ ,  $\delta_S$ ,  $\mu_S$ ,  $\mu_L$ ) from one immunization to the following one, eventually also based on the time between the two doses. In particular, an improved antibody response has been experimentally observed when the delay between the first and second doses is higher (e.g. 56 days schedule compared to 28 days). Therefore, according to sensitivity analysis performed in Section 6, we suggest to investigate through modeling the possibility of an increase of parameters  $\rho$  and  $\mu_L$  when increasing the time lapse between the two doses, the opposite for parameters  $\mu_S$  and  $\delta_S$ . Note that the effect of timing of the second dose on the half-life of short-lived ASCs has been already observed by Pasin and coauthors (Pasin et al., 2019).

Moreover, due to (MSL) definition, if we do not change any parameter among  $\{\rho, \mu_L, \mu_S\}$  from the first to following doses, BMEMs level remains almost unchanged (Section 3.3), while we expect an increase in the concentration of BMEMs after the booster dose.

After vaccination, the existence of a plateau reached by functional persisting BMEMs has been reported in the literature (Crotty et al., 2003). In (MSL) this plateau is quickly reached, due to the fact that we do not consider here any intermediate maturation step from naïve to activated to functional differentiated cells: when the antigen is introduced in the system, the  $M$  compartment is almost instantaneously filled. The main consequence is that the contribution of this compartment to enhance the secondary response will be substantially unchanged regardless the time delay between two subsequent vaccine immunizations, in the situation in which no parameter modification is permitted.

Despite the simplifications in model structure, several identifiability issues have been raised in Sections 4 and 6. Consequently, another limitation of this study is that model parameters could not be accurately and univocally determined.

The (MSL) model provides a good starting point to evaluate the humoral immune response elicited by the proposed vaccination regimens. Several future research directions can be suggested by this work. For instance, (MSL) model can be further refined using future data that will be available from ongoing phase II and III clinical studies, in particular regarding B cell populations and immune response after a booster vaccination. Other questions should be addressed *in silico*. In particular, (MSL) model could be generalized by relaxing the assumption of replication deficient vaccine vectors to allow the study of the immune response elicited by live attenuated vaccine virus. Indeed, it would be interesting to test (MSL) with other vaccination studies, to determine whether some parameters are independent from the type of vaccine vector used.

## 9. Conclusion

In this work we set a mechanistic model - (MSL)- of the humoral immune response to one or more vaccine immunizations, based on an ODE system of 5 equations. It describes the interaction between the antigen delivered by replication deficient vaccine vectors, BMEMs, ASCs (distinguishing two populations differing by their respective half-lives) and produced antigen-specific antibodies. We have analyzed model structure identifying which kind of biological data should be collected or alternatively which parameters should be fixed to perform proper parameter estimations. By confronting (MSL) with ELISA data from two-dose heterologous vaccination regimens against Ebola virus, we show that the model is able to reproduce realistic antibody concentration dynamics after the two-dose heterologous vaccination. This provides the rationale to test the ability of (MSL) in predicting the speed and magnitude of the immune response to a booster vaccine dose, as we show in this paper, and investigate long-term antibody persistence. Our findings raise interesting further questions. Some of them require further biological data, in particular regarding B cell populations assessment. Also, one could be interested in understanding if some model parameters are intrinsic properties of the immune response, hence could help describing the response to natural infection. Other questions should be addressed *in silico* to explore the interaction of additional immune components and their contribution to the establishment, maintenance and reactivation of the immune response to a repeatedly presented antigen.

## CRediT authorship contribution statement

**Irene Balelli:** Conceptualization, Methodology, Software, Formal analysis, Writing - original draft, Writing - review & editing. **Chloé Pasin:** Conceptualization, Methodology, Writing - review & editing. **Mélanie Prague:** Conceptualization, Writing - review & editing. **Fabien Crauste:** Writing - review & editing. **Thierry Van Effelterre:** Writing - review & editing. **Viki Bockstal:** Data curation, Writing - review & editing. **Laura Solforosi:** Data curation, Writing - review & editing. **Rodolphe Thiébaud:** Conceptualization, Supervision, Writing - review & editing.

## Acknowledgments

We thank the members of the EBOVAC1 consortium, in particular the principal investigators of the EBOVAC1 trials, Matthew Snape, Omu Anzala, George Praygod, Zacchaeus Anywaine. We also thank Andrew Pollard and Elizabeth Clutterbuck for scientific discussions.

In addition, we thank the members of the EBOVAC3 consortium and in particular Rosalind Eggo, Niel Hens, Carl Pearson and Bart Spiessens, involved in the modeling effort supporting the development of the two-dose heterologous regimen developed by Janssen Vaccines & Prevention B.V., and discussed in this paper.

This work has received funding from the Innovative Medicines Initiative 2 Joint Undertaking under Grant Agreement EBOVAC1 (No. 115854). This Joint Undertaking receives support from the European Union's Horizon 2020 research and innovation programme and EFPIA. The funder of the study had no role in the study design, data collection, data analysis, data interpretation, or writing the report. The corresponding author had full access to all the data in the study and had final responsibility for the decision to submit for publication. This work was also supported by the Investissements d'Avenir program managed by the ANR under reference ANR-10-LABX-77. The funder had no role in the study design, data collection, data analysis, data interpretation, or writing the report.

Competing interests: TVE, VB and LS are employees of Janssen Pharmaceuticals and may be Johnson & Johnson stockholders.

## Appendix A. The IdentifiabilityAnalysis package

In order to assess the *a priori* local structural identifiability of (MSL) we use the Exact Arithmetic Rank (EAR) approach implemented in Mathematica through the IdentifiabilityAnalysis package (Karlsson et al., 2012). It is the Mathematica implementation of a probabilistic semi-numerical algorithm described in Sedoglavic (2001) based on rank computation of a numerically instantiated Jacobian matrix. This is called the rank test for structural identifiability (Pohjanpalo, 1978).

## Appendix B. Matlab function sens\_ind for numerical evaluation of partial derivatives

To evaluate the first-order partial derivatives of model outputs with respect to its parameters around a local point in the parameter space, we use Matlab function sens\_ind (Victor M. Garcia-Molla, 2017). It is based on Matlab function ode15 and is able to compute the derivatives of an ODE system with respect to its parameters, by using the *Internal Numerical Differentiation* approach (Bock, 1981).

## Supplementary material

Supplementary material associated with this article can be found, in the online version, at doi:10.1016/j.jtbi.2020.110254.

## References

- Ademokun, A.A., Dunn-Walters, D., 2010. Immune responses: primary and secondary. *Encyclop. Life Sci.*
- Andraud, M., Lejeune, O., Musoro, J.Z., Ogunjimi, B., Beutels, P., Hens, N., 2012. Living on three time scales: the dynamics of plasma cell and antibody populations illustrated for hepatitis a virus. *PLoS Comput. Biol.* 8 (3), e1002418.
- Antia, R., Bergstrom, C.T., Pilyugin, S.S., Kaech, S.M., Ahmed, R., 2003. Models of CD8+ responses: 1. what is the antigen-independent proliferation program. *J. Theor. Biol.* 221 (4), 585–598. doi:10.1006/jtbi.2003.3208.
- Anywine, Z., Whitworth, H., Kaleebu, P., Praygod, G., Shukarev, G., Manno, D., Kapiga, S., Grosskurth, H., Kalluvya, S., Bockstal, V., et al., 2019. Safety and immunogenicity of a 2-dose heterologous vaccination regimen with Ad26. ZEBOV and MVA-BN-Filo Ebola vaccines: 12-month data from a phase 1 randomized clinical trial in uganda and tanzania. *J. Infect. Dis.* 220 (1), 46–56.
- Belshe, R.B., Frey, S.E., Graham, I., Mulligan, M.J., Edupuganti, S., Jackson, L.A., Wald, A., Poland, G., Jacobson, R., Keyserling, H.L., et al., 2011. Safety and immunogenicity of influenza a h5 subunit vaccines: effect of vaccine schedule and antigenic variant. *J. Infect. Dis.* 203 (5), 666–673.
- Bock, H.G., 1981. Numerical treatment of inverse problems in chemical reaction kinetics. In: *Modelling of chemical reaction systems*. Springer, pp. 102–125.
- Callendret, B., Vellinga, J., Wunderlich, K., Rodriguez, A., Steigerwald, R., Dirmeier, U., Cheminay, C., Volkman, A., Brasel, T., Carrion, R., et al., 2018. A prophylactic multivalent vaccine against different filovirus species is immunogenic and provides protection from lethal infections with ebolavirus and marburgvirus species in non-human primates. *PLoS ONE* 13 (2), e0192312.
- Carter, M.J., Mitchell, R.M., Meyer Sauter, P.M., Kelly, D.F., Trück, J., 2017. The antibody-secreting cell response to infection: kinetics and clinical applications. *Front. Immunol.* 8, 630.
- Crotty, S., Felgner, P., Davies, H., Glidewell, J., Villarreal, L., Ahmed, R., 2003. Cutting edge: long-term B cell memory in humans after smallpox vaccination. *J. Immunol.* 171 (10), 4969–4973.
- Davis, C.L., Wahid, R., Toapanta, F.R., Simon, J.K., Szein, M.B., 2018. A clinically parameterized mathematical model of shigella immunity to inform vaccine design. *PLoS ONE* 13 (1), e0189571.
- De Boer, R.J., Oprea, M., Antia, R., Ahmed, R., Perelson, A.S., Murali-krishna, K., 2001. Recruitment times, proliferation, and apoptosis rates during the CD8+ t-cell response to lymphocytic choriomeningitis virus. *J. Virol.* doi:10.1128/JVI.75.22.10663.
- De Silva, N.S., Klein, U., 2015. Dynamics of B cells in germinal centres. *Nat. Rev. Immunol.* 15 (3), 137.
- Dye, J.M., Herbert, A.S., Kuehne, A.I., Barth, J.F., Muhammad, M.A., Zak, S.E., Ortiz, R.A., Prugar, L.I., Pratt, W.D., 2012. Postexposure antibody prophylaxis protects nonhuman primates from filovirus disease. *Proc. Natl. Acad. Sci.* 109 (13), 5034–5039.
- Ebovac2, 2018. 7th Ebovac2 e-newsletter. [http://www.ebovac2.com/images/EBOVAC2\\_newsletter7\\_19112018.pdf](http://www.ebovac2.com/images/EBOVAC2_newsletter7_19112018.pdf), Last accessed on 2020-01-31.
- Eurosurveillance editorial team, 2015. First innovative medicines initiative ebola projects launched. *Eurosurveillance* 20 (3), 21014.
- Farber, D.L., Netea, M.G., Radbruch, A., Rajewsky, K., Zinkernagel, R.M., 2016. Immunological memory: lessons from the past and a look to the future. *Nat. Rev. Immunol.* 16 (2), 124.
- Fraser, C., Tomassini, J.E., Xi, L., Golm, G., Watson, M., Giuliano, A.R., Barr, E., Ault, K.A., 2007. Modeling the long-term antibody response of a human papillomavirus (hpv) virus-like particle (vlp) type 16 prophylactic vaccine. *Vaccine* 25 (21), 4324–4333.
- Goldstein, T., Anthony, S.J., Gbakima, A., Bird, B.H., Bangura, J., Tremereau-Bravard, A., Belaganahalli, M.N., Wells, H.L., Dhanota, J.K., Liang, E., et al., 2018. The discovery of bombali virus adds further support for bats as hosts of ebolaviruses. *Nat. Microbiol.* 3 (10), 1084.
- Green, C., Sande, C., De Lara, C., Thompson, A., Silva-Reyes, L., Napolitano, F., Pierantonio, A., Capone, S., Vitelli, A., Klennerman, P., et al., 2018. Humoral and cellular immunity to rsv in infants, children and adults. *Vaccine* 36 (41), 6183–6190.
- Gross, L., Lhomme, E., Pasin, C., Richert, L., Thiebaut, R., 2018. Ebola vaccine development: systematic review of pre-clinical and clinical studies, and meta-analysis of determinants of antibody response variability after vaccination. *Int. J. Infectious Dis.* 74, 83–96.
- Guedj, J., Thiébaut, R., Commenges, D., 2007. Maximum likelihood estimation in dynamical models of HIV. *Biometrics* 63 (4), 1198–1206.
- Halliley, J.L., Kyu, S., Kobie, J.J., Walsh, E.E., Falsey, A.R., Randall, T.D., Treanor, J., Feng, C., Sanz, I., Lee, F.E.-H., 2010. Peak frequencies of circulating human influenza-specific antibody secreting cells correlate with serum antibody response after immunization. *Vaccine* 28 (20), 3582–3587.
- Halliley, J.L., Tipton, C.M., Liesveld, J., Rosenberg, A.F., Darce, J., Gregoret, I.V., Popova, L., Kaminiski, D., Fucile, C.F., Albizua, I., et al., 2015. Long-lived plasma cells are contained within the cd19+ cd38hicd138+ subset in human bone marrow. *Immunity* 43 (1), 132–145.
- Hammarlund, E., Thomas, A., Amanna, I.J., Holden, L.A., Slayden, O.D., Park, B., Gao, L., Slifka, M.K., 2017. Plasma cell survival in the absence of B cell memory. *Nat. Commun.* 8 (1), 1781.
- Hanke, T., McMichael, A.J., Dennis, M.J., Sharpe, S.A., Powell, L.A., McLoughlin, L., Crome, S.J., 2005. Biodistribution and persistence of an mva-vectored candidate HIV vaccine in SIV-infected rhesus macaques and SCID mice. *Vaccine* 23 (12), 1507–1514.
- Hartman, P., Olech, C., 1962. On global asymptotic stability of solutions of differential equations. *Trans. Am. Math. Soc.* 104 (1), 154–178.
- Hviid, L., Barfod, L., Fowkes, F.J., 2015. Trying to remember: immunological B cell memory to malaria. *Trends Parasitol.* 31 (3), 89–94.
- Inoue, T., Moran, I., Shinnakasu, R., Phan, T.G., Kurosaki, T., 2018. Generation of memory B cells and their reactivation. *Immunol. Rev.* 283 (1), 138–149.
- Jilg, W., Schmidt, M., Deinhardt, F., 1989. Vaccination against hepatitis b: comparison of three different vaccination schedules. *J. Infect. Dis.* 160 (5), 766–769.
- Jones, D.D., Wilmore, J.R., Allman, D., 2015. Cellular dynamics of memory B cell populations: IgM+ and IgG+ memory B cells persist indefinitely as quiescent cells. *J. Immunol.* 195(13), 3655–3665.
- Karlsson, J., Angelova, M., Jirstrand, M., 2012. An efficient method for structural identifiability analysis of large dynamic systems. *IFAC Proc. Vol.* 45 (16), 941–946.
- Lavielle, M., Aarons, L., 2016. What do we mean by identifiability in mixed effects models? *J. Pharmacokinet. Pharmacodyn.* 43 (1), 111–122.
- Le, D., Miller, J.D., Ganusov, V.V., 2015. Mathematical modeling provides kinetic details of the human immune response to vaccination. *Front. Cell. Infect. Microbiol.* 4, 177.
- Leach, S., Lundgren, A., Svennerholm, A.-M., 2013. Different kinetics of circulating antibody-secreting cell responses after primary and booster oral immunizations: a tool for assessing immunological memory. *Vaccine* 31 (30), 3035–3038.
- Lessler, J., Riley, S., Read, J.M., Wang, S., Zhu, H., Smith, G.J., Guan, Y., Jiang, C.Q., Cummings, D.A., 2012. Evidence for antigenic seniority in influenza a (h3n2) antibody responses in southern china. *PLoS Pathog.* 8 (7).
- Li, G.-M., Chiu, C., Wrammert, J., McCausland, M., Andrews, S.F., Zheng, N.-Y., Lee, J.-H., Huang, M., Qu, X., Edupuganti, S., et al., 2012. Pandemic h1n1 influenza vaccine induces a recall response in humans that favors broadly cross-reactive memory b cells. *Proc. Natl. Acad. Sci.* 109 (23), 9047–9052.
- Miao, H., Xia, X., Perelson, A.S., Wu, H., 2011. On identifiability of nonlinear ode models and applications in viral dynamics. *SIAM Rev.* 53 (1), 3–39.
- Milligan, I.D., Gibani, M.M., Sewell, R., Clutterbuck, E.A., Campbell, D., Plested, E., Nuthall, E., Voysey, M., Silva-Reyes, L., McElrath, M.J., et al., 2016. Safety and immunogenicity of novel adenovirus type 26-and modified vaccinia ankara-vectored ebola vaccines: a randomized clinical trial. *JAMA* 315 (15), 1610–1623.
- Mutua, G., Anzala, O., Luhn, K., Robinson, C., Bockstal, V., Anumendem, D., Douguhi, M., 2019. Safety and immunogenicity of a 2-dose heterologous vaccine regimen with ad26. ZEBOV and MVA-BN-Filo ebola vaccines: 12-month data from a phase 1 randomized clinical trial in nairobi, kenya. *J. Infect. Dis.* 220 (1), 57–67.
- Nommensen, F., Go, S., MacLaren, D., 1989. Half-life of hbs antibody after hepatitis b vaccination: an aid to timing of booster vaccination. *The Lancet* 334 (8667), 847–849.
- World Health Organisation, et al., 2016. Situation report: Ebola virus disease, 10 june 2016. World Health Organization, Geneva.
- World Health Organisation, et al., 2018. Ebola situation reports: Democratic republic of the congo.

- Pasin, C., Balelli, I., Van Effelterre, T., Bockstal, V., Solforosi, L., Prague, M., Douoguih, M., Thiébaud, R., 2019. Dynamics of the humoral immune response to a prime-boost ebola vaccine: quantification and sources of variation. *J. Virol.* doi:10.1128/JVI.00579-19.
- Pohjanpalo, H., 1978. System identifiability based on the power series expansion of the solution. *Math. Biosci.* 41 (1–2), 21–33.
- Prague, M., Commenges, D., Guedj, J., Drylewicz, J., Thiébaud, R., 2013. Nimrod: a program for inference via a normal approximation of the posterior in models with random effects based on ordinary differential equations. *Comput. Method. Progr. Biomed.* 111 (2), 447–458.
- Pulendran, B., Ahmed, R., 2006. Translating innate immunity into immunological memory: implications for vaccine development. *Cell* 124 (4), 849–863.
- van Ravenhorst, M.B., Marinovic, A.B., van der Klis, F.R., van Rooijen, D.M., van Maurik, M., Stoof, S.P., Sanders, E.A., Berbers, G.A., 2016. Long-term persistence of protective antibodies in dutch adolescents following a meningococcal serogroup c tetanus booster vaccination. *Vaccine* 34 (50), 6309–6315.
- Sallusto, F., Lanzavecchia, A., Araki, K., Ahmed, R., 2010. From vaccines to memory and back. *Immunity* 33 (4), 451–463.
- Sedoglavic, A., 2001. A probabilistic algorithm to test local algebraic observability in polynomial time. In: *Proceedings of the 2001 international symposium on Symbolic and algebraic computation*. ACM, pp. 309–317.
- Shah, H.B., Koelsch, K.A., 2015. B-Cell Elispot: For the Identification of Antigen-specific Antibody-secreting Cells. In: *Western Blotting*. Springer, pp. 419–426.
- Sheets, R.L., Stein, J., Bailer, R.T., Koup, R.A., Andrews, C., Nason, M., He, B., Koo, E., Trotter, H., Duffy, C., et al., 2008. Biodistribution and toxicological safety of adenovirus type 5 and type 35 vectored vaccines against human immunodeficiency virus-1 (hiv-1), ebola, or marburg are similar despite differing adenovirus serotype vector, manufacturer's construct, or gene inserts. *J. Immunotoxicol.* 5 (3), 315–335.
- Shlomchik, M.J., 2018. Do memory B cells form secondary germinal centers? yes and no. *Cold Spring Harb. Perspect. Biol.* 10 (1), a029405.
- Sullivan, N.J., Martin, J.E., Graham, B.S., Nabel, G.J., 2009. Correlates of protective immunity for ebola vaccines: implications for regulatory approval by the animal rule. *Nat. Rev. Microbiol.* 7 (5), 393.
- Tangye, S.G., Avery, D.T., Deenick, E.K., Hodgkin, P.D., 2003. Intrinsic differences in the proliferation of naive and memory human B cells as a mechanism for enhanced secondary immune responses. *J. Immunol.* 170 (2), 686–694.
- Team, W.E.R., 2016. After ebola in west africa - unpredictable risks, preventable epidemics. *N. Top N. Engl. J. Med.* 375 (6), 587–596.
- Teunis, P., Van Der Heijden, O., De Melker, H., Schellekens, J., Versteegh, F., Kretzschmar, M., 2002. Kinetics of the IgG antibody response to pertussis toxin after infection with b. pertussis. *Epidemiol. Infect.* 129 (3), 479–489.
- Van Herck, K., Van Damme, P., 2001. Inactivated hepatitis a vaccine-induced antibodies: follow-up and estimates of long-term persistence. *J. Med. Virol.* 63 (1), 1–7.
- Van Twillert, I., Marinović, A.A.B., Kuipers, B., Sanders, E.A., van Els, C.A., et al., 2017. Impact of age and vaccination history on long-term serological responses after symptomatic b. pertussis infection, a high dimensional data analysis. *Sci. Rep.* 7, 40328.
- Venkatraman, N., Silman, D., Folegatti, P.M., Hill, A.V., 2018. Vaccines against ebola virus. *Vaccine* 36 (36), 5454–5459.
- Victor M. Garcia-Molla, 2017. Sensitivity analysis for odes and daes, MATLAB Central File Exchange. <https://fr.mathworks.com/matlabcentral/fileexchange/1480-sensitivity-analysis-for-odes-and-daes>, Retrieved on 2017-09-07.
- Victora, G.D., Nussenzweig, M.C., 2012. Germinal centers. *Annu. Rev. Immunol.* 30, 429–457.
- White, M.T., Griffin, J.T., Akpogheneta, O., Conway, D.J., Koram, K.A., Riley, E.M., Ghani, A.C., 2014. Dynamics of the antibody response to plasmodium falciparum infection in african children. *J. Infect. Dis.* 210 (7), 1115–1122.
- Wilson, J.N., Nokes, D.J., 1999. Do we need 3 doses of hepatitis b vaccine? *Vaccine* 17 (20), 2667–2673.
- Wilson, J.N., Nokes, D.J., Medley, G.F., Shouval, D., 2007. Mathematical model of the antibody response to hepatitis b vaccines: implications for reduced schedules. *Vaccine* 25 (18), 3705–3712.
- Winslow, R.L., Milligan, I.D., Voysey, M., Luhn, K., Shukarev, G., Douoguih, M., Snape, M.D., 2017. Immune responses to novel adenovirus type 26 and modified vaccinia virus ankara-vectored ebola vaccines at 1 year. *JAMA* 317 (10), 1075–1077.
- Wong, G., Richardson, J.S., Pillet, S., Patel, A., Qiu, X., Alimonti, J., Hogan, J., Zhang, Y., Takada, A., Feldmann, H., et al., 2012. Immune parameters correlate with protection against ebola virus infection in rodents and nonhuman primates. *Sci. Transl. Med.* 4 (158), 158ra146–158ra146.
- World Health Organisation, 2018. Ebola virus disease, Fact Sheet. <https://www.who.int/news-room/fact-sheets/detail/ebola-virus-disease>, Last accessed on 2019-05-04.
- World Health Organisation, 2019a. Ebola virus disease, Democratic Republic of the Congo, External Situation Report N°82/2019. <https://www.who.int/publications-detail/ebola-virus-disease-democratic-republic-of-congo-external-situation-report-82-2019>, Last accessed on 2020-03-05.
- World Health Organisation, 2019b. Statement on the meeting of the International Health Regulations (2005) Emergency Committee for Ebola virusdisease in the Democratic Republic of the Congo on 17 July 2019. <https://www.who.int/ihr/procedures/statement-emergency-committee-ebola-drc-july-2019.pdf>, Last accessed on 2019-07-23.
- Zi, Z., 2011. Sensitivity analysis approaches applied to systems biology models. *IET Syst. Biol.* 5 (6), 336–346.